Modified Virtual Oscillator-Based Operation of Grid-Forming Converters with Single Voltage Sensor

Preprint

Vikram Roy Chowdhury, Akanksha Singh, and Barry Mather

National Renewable Energy Laboratory

Presented at the IEEE Energy Conversion Congress & Exposition (ECCE)
Nashville, Tennessee
October 29–November 2, 2023

NREL is a national laboratory of the U.S. Department of Energy
Office of Energy Efficiency & Renewable Energy
Operated by the Alliance for Sustainable Energy, LLC

This report is available at no cost from the National Renewable Energy Laboratory (NREL) at www.nrel.gov/publications.

Contract No. DE-AC36-08GO28308

Conference Paper
NREL/CP-5D00-85362
November 2024

Modified Virtual Oscillator-Based Operation of Grid-Forming Converters with Single Voltage Sensor

Preprint

Vikram Roy Chowdhury, Akanksha Singh, and Barry Mather

National Renewable Energy Laboratory

Suggested Citation
Roy Chowdhury, Vikram, Akanksha Singh, and Barry Mather. 2023. *Modified Virtual Oscillator-Based Operation of Grid-Forming Converters with Single Voltage Sensor: Preprint*. Golden, CO: National Renewable Energy Laboratory. NREL/CP-5D00-85362. https://www.nrel.gov/docs/fy24osti/85362.pdf.

NREL is a national laboratory of the U.S. Department of Energy
Office of Energy Efficiency & Renewable Energy
Operated by the Alliance for Sustainable Energy, LLC

This report is available at no cost from the National Renewable Energy Laboratory (NREL) at www.nrel.gov/publications.

Contract No. DE-AC36-08GO28308

Conference Paper
NREL/CP-5D00-85362
November 2024

National Renewable Energy Laboratory
15013 Denver West Parkway
Golden, CO 80401
303-275-3000 • www.nrel.gov

NOTICE

This work was authored by the National Renewable Energy Laboratory, operated by Alliance for Sustainable Energy, LLC, for the U.S. Department of Energy (DOE) under Contract No. DE-AC36-08GO28308. Funding provided by U.S. Department of Energy Office of Energy Efficiency and Renewable Energy Solar Energy Technologies Office. The views expressed herein do not necessarily represent the views of the DOE or the U.S. Government.

Cover Photos by Dennis Schroeder: (clockwise, left to right) NREL 51934, NREL 45897, NREL 42160, NREL 45891, NREL 48097, NREL 46526.

NREL prints on paper that contains recycled content.

Modified Virtual Oscillator-Based Operation of Grid-Forming Converters with Single Voltage Sensor

Vikram Roy Chowdhury
National Renewable Energy Laboratory
Golden, CO, USA
vikram.roychowdhury@nrel.gov

Akanksha Singh
Principal Engineer - Power Conversion
DNV, USA
akanksha.singh@dnv.com

Barry Mather
National Renewable Energy Laboratory
Golden, CO, USA
barry.mather@nrel.gov

***Abstract*—This paper proposes a virtual oscillator-based control architecture for a grid-forming converter with an inner current control loop. In general, the virtual oscillator is based on a Lienard type of oscillator equation with a cubic nonlinearity. A virtual oscillator alone cannot accommodate unbalanced or harmonic mitigation while operating converters in grid-forming mode. Therefore, to accomplish better tracking performance, incorporating the provision for nonlinear and/or unbalanced loads, an inner current control loop is utilized that is based on the Lyapunov energy function type control architecture. To reduce the overall cost of implementation and ensure proper phase difference in the generated voltages, the implemented virtual oscillator operates with only one voltage feedback from the point of common coupling. To verify the effectiveness of the proposed approach, the overall system has been modeled in MATTLAB/Simulink and PLECS domain. This paper also presents case studies showing the successful production of low harmonic load voltages under nonideal loading conditions, along with other important results.**

***Index Terms*—Three-phase grid forming inverter, Nonlinear/ unbalanced loads, Single voltage sensor, Dual second order generalized integrator ($DSOGI$), Photovoltaic (PV) system, Point of common coupling (PCC).**

I. Introduction

THE focus on reducing dependence on fossil fuel for power production has enabled the usage of renewable energy resources like PV or wind energy in recent years [1]–[7]. The most commonly used renewable resource is PV for power conversion due to its abundance and easy availability. However, power available from a PV generation system is highly intermittent and a function of the solar potential or irradiation, moisture, weather conditions, etc. Therefore, to operate the overall system in the most optimal manner, advanced control architecture is needed [8]–[11]. Several control architectures for PV converters have been reported in various literature based on virtual synchronous machines (VSM), direct power control (DPC), virtual oscillators (VO), etc. [12]–[14]. VSM or synchronverters are converters that are operated in a manner to emulate the mechanical dynamics of a synchronous machine. This ensures a virtual inertia to disturbances from the point of common coupling (PCC), mostly in the frequency. However, VSM suffers from two major issues: (1) the attainable bandwidth for this type of control is low, which slows the operation of the converter, and (2) traditional VSM cannot operate under PCC unbalance/distortion and needs additional control loops to cater this problem, which thereby enhances the complexity of the overall system [6]. Traditional VSM-based control architecture has a very slow response to reactive power support based on the non-minimum phase behavior of the reactive power loop [15]. The DPC architecture is based on the control of the overall system, based on computation of the power to be transferred from the converter to the PCC. Several architectures for DPC have been presented in literature [16]–[18]. However, DPC similar to VSM needs either the information of the PCC voltage, which can be accomplished using a phase locked loop (PLL), or if the system is operating without a PLL like a VSM it requires a startup scheme to be connected to the PCC in order to avoid huge current spikes, resulting in protection circuit to trip the overall system.

In this paper, a virtual oscillator (VO)-based control architecture is investigated, which is based on nonlinear oscillators proven to accomplish stable limit cycle when certain conditions are met, as presented in [14], [19]. VO-based architecture dynamics are used to generate the references for the inner current control loops based on a Lyapunov energy function, which has been utilized in this work for better tracking performance as well as to accommodate operation under nonideal PCC conditions. Lyapunov energy function-based architectures have already been presented in various literature [10], [11], [20], [21] for grid-forming as well as grid-

This work was authored by the National Renewable Energy Laboratory, operated by Alliance for Sustainable Energy, LLC, for the U.S. Department of Energy (DOE) under Contract No. DE-AC36-08GO28308. Funding provided by U.S. Department of Energy Office of Energy Efficiency and Renewable Energy Solar Energy Technologies Office. The views expressed in the article do not necessarily represent the views of the DOE or the U.S. Government.

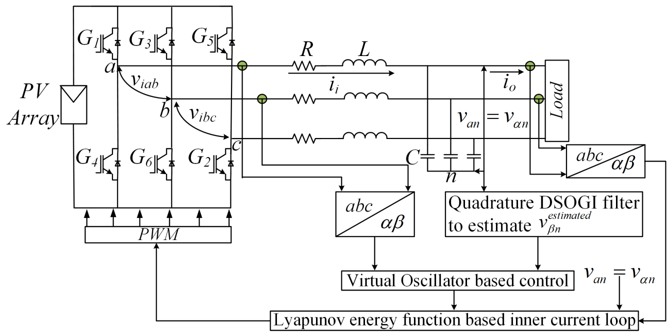

Fig. 1: Implementation of modified VO with inner current and voltage control loops for better operational capabilities

following applications. However, a Lyapunov energy function-based control architecture using VO as the outer loop to generate the necessary dynamics as well as references has not been reported in any literature. It is reported in [14], [19] that operating VO for three-phase application requires generation of proper phase shifted voltage waveform, which with traditional architecture is challenging. Therefore, in this work, at the converter level the generation of voltage is accomplished at one of the phases of the converter, and the other phases are generated by proper phase shifting. Such an architecture has the advantage of reduced number of sensors—consequently, a lower implementation cost. However, this architecture also introduce non-negligible dynamics for the generation of the phase voltage waveform, which in turn limits the attainable bandwidth of the overall control architecture.

The rest of the paper is organized as follows: Section II presents the step by step derivation of the virtual oscillator-based control architecture with inner Lyapunov energy function-based control loops, Section III presents the need and methodology to estimate the other voltage components, Section IV presents the results and discussion, followed by a conclusion in Section V.

II. Step by Step Derivation of the Virtual Oscillator-Based Control Architecture with Inner Current and Voltage Control

In this section, modified VO-based control of grid-forming converter is derived and presented. The concept of VO is based on a nonlinear Lienard type of oscillators as presented in [14], [19], where the electrical equivalent of the circuit is presented by a parallel resonant RLC circuit with dependent voltage and/or current sources. This paper presents the possibility of using this concept for grid-forming methodology, where the primary objective is to obtain low harmonic voltage at the PCC under nonlinear and/or unbalanced loading conditions. The mathematical model of a standard VO is presented in [14], [19], where the nonlinear functions are defined elaborately. The per-phase electrical equivalent of the VO-based control presented in Fig. 1 has been elaborated in Fig. 2. It is observed from Fig. 1 that only one ac voltage $v_{an} = v_{\alpha n}$ has been sensed. The quadrature filter

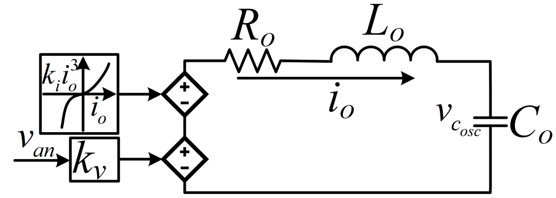

Fig. 2: Series RLC equivalent of the virtual oscillator

for a dual second order generalized integrator ($DSOGI$) [22] architecture is used inside the VO to estimate the β axis voltage. The series RLC equivalent of the VO is presented in Fig. 2. More details along with the block diagram of the β axis voltage estimation via $DSOGI$ architecture are presented in the next section.

$$\ddot{i}_o + \varepsilon f(i_o)\,\dot{i}_o + \omega^2 i_o = \varepsilon\omega\,\dot{u}(t) \tag{1}$$

The VO of Fig. 2 consists of two dependent voltage sources, the inputs to which are the actual ac circuit voltage and a nonlinear function of the series RLC circuit current $g(i_o) = k_i i_o^3$. The oscillator output voltage $v_{c_{osc}}$ is used as the reference for the inner current control loop based on a Lyapunov energy function. Dynamics of the VO is presented in (1), which is in the standard Lienard form as presented in [14], [19]. In (1), $\epsilon = \sqrt{\frac{1}{L_o}}$, $\omega = \sqrt{\frac{1}{L_o C_o}}$, $f(i_o) = \sqrt{\frac{1}{L_o}}(\frac{R_o - 3k_i i_o^2}{\sqrt{L_o}})$, k_v and k_i are user defined constants based on the gains between the sensing circuit and the microcontroller, $u(t) = v_{an}$. A VO-based control architecture with time domain incorporates droop within itself as presented in [14], [19]. Therefore, successful power sharing when several of these are connected in parallel to form a microgrid can also be accomplished. In this paper, to accomplish better operation capability, an inner control loop based on the Lyapunov energy function [10] has been implemented due to its reported advantages [11], [20], [21]. To reduce the number of equations, the inner loop is accomplished in a stationary two-phase ($\alpha\beta$) domain. Considering symmetry, only the α axis dynamics are presented. Similar expressions can also be obtained for the β axis. The dynamics of the capacitor voltage and the inductor current are presented in (2) and (3), respectively, for the reference and the actual quantities.

$$\begin{aligned} L\frac{di_{i\alpha}^{ref}}{dt} &= -Ri_{i\alpha}^{ref} + m_{\alpha}^{ref} \quad \frac{V_{dc}}{2} - v_{\alpha n}^{ref} \\ C\frac{dv_{\alpha n}^{ref}}{dt} &= i_{i\alpha}^{ref} - i_{o\alpha}^{ref} \end{aligned} \tag{2}$$

$$\begin{aligned} L\frac{di_{i\alpha}}{dt} &= -Ri_{i\alpha} + m_{\alpha} \quad \frac{V_{dc}}{2} - v_{\alpha n} \\ C\frac{dv_{\alpha n}}{dt} &= i_{i\alpha} - i_{o\alpha} \end{aligned} \tag{3}$$

$$\begin{aligned} L\frac{dx_1}{dt} &= -Rx_1 + \Delta m_{\alpha} \quad \frac{V_{dc}}{2} - x_2 \\ C\frac{dx_2}{dt} &= x_1 \end{aligned} \tag{4}$$

Define: $x_1 = v_{\alpha n} - v_{\alpha n}^{ref}$ and $x_2 = i_{i\alpha} - i_{i\alpha}^{ref}$. Considering sine pulse width modulation (PWM), the instantaneous inverter voltage can be defined as $v_{i\alpha} = m_{\alpha}\frac{V_{dc}}{2}$. Using these definitions, the error dynamics of the overall system is presented in (4), where $\Delta m = m_\alpha - m_\alpha^{ref}$. An energy function based on these errors satisfying all the criteria presented in [10] is defined as presented in (5). Differentiating (5) with respect to time, we have:

$$V = \frac{1}{2}Lx_1^2 + \frac{1}{2}Cx_2^2 \tag{5}$$

$$\dot{V} = -Rx_1^2 + x_1\Delta m_\alpha \frac{V_{dc}}{2} \tag{6}$$

Equation (6) satisfies all the criteria to ensure negative definiteness as per the definition with the choice of $\Delta m_\alpha = -\frac{2R_c}{V_{dc}}x_1$. Therefore, the overall control law is obtained and is given by $m_\alpha = m_\alpha^{ref} + \Delta m_\alpha = \frac{2}{V_{dc}}\left(L\frac{di_{i\alpha}^{ref}}{dt} + Ri_{i\alpha}^{ref} + v_{\alpha n}^{ref}\right) + R_c\left(i_{i\alpha}^{ref} - i_{i\alpha}\right)$ where $R_c > 0$ is the Lyapunov energy function-based gain and is a user input. The reference inductor current for a specified capacitor voltage is given by $i_{i\alpha}^{ref} = i_{o\alpha}^{ref} + C\frac{dv_{\alpha n}^{ref}}{dt}$ with $v_{\alpha n}^{ref} = v_{c_{osc}}$. The next section shows the methodology and utility for estimating the β axis voltage for the inner loop using the sensed voltage from the PCC.

III. Methodology for Voltage Estimation

The methodology to estimate the β axis voltage from the sensed PCC voltage is elaborated in this section. The quadrature filter for the $DSOGI$ architecture has been utilized to estimate the β axis terminal voltage. It has been presented in [14], [19] that the voltage generated from a VO is a function of initial condition for both the magnitude and phase. Therefore, to accomplish the implementation of the VO in α and β axes, precise choice of initial condition to accomplish 90^o phase shift between the generated voltages is a necessary prerequisite. However, having such precise initial condition becomes an immense challenge to accomplish as this would require solving the circuit equation every time the interrupt activates the sensing circuit and new data is obtained to the overall controller code. Therefore, to avoid such an issue, in this paper, the α axis PCC voltage is sensed and the β axis is estimated. The sensed ac voltage is $v_{an} = v_{\alpha n}$ as presented in Fig. 1, which is true for $\alpha\beta$ domain with proper phase orientation where β axis leads α. As mentioned earlier, the $DSOGI$ architecture's quadrature filter is used to generate the β axis voltage as shown in Fig. 3, whose mathematical expression is presented in (7).

$$G_{quad} = \frac{K\omega^2}{s^2 + K\omega s + \omega^2} \tag{7}$$

where K is the damping coefficient, and ω is the PCC frequency. The input to the filter is the sensed PCC voltage, and the output is the quadrature voltage, which can be used as the β axis voltage for the controller architecture. The step response of the estimator is presented in Fig. 3. It is observed from this result that the filter architecture is able to generate the quadrature axis voltage successfully with the chosen bandwidth and with zero attenuation of the signal. The parameters of the quadrature filter and other control parameters are presented in Table I. The generated β axis voltage is used for the inner loop, and the overall controller is implemented. The next section presents the verification of the overall system via computer simulations for important case studies.

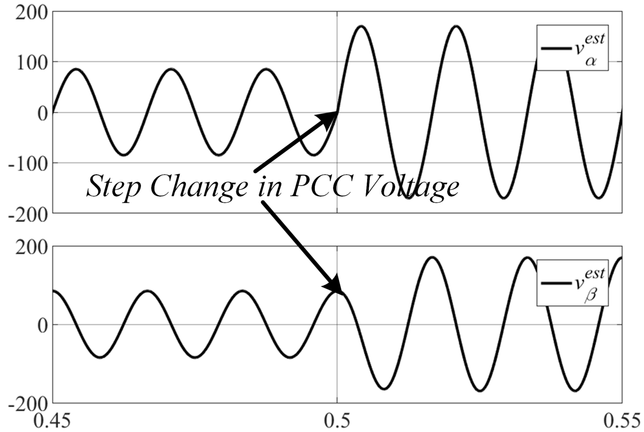

Fig. 3: Dynamic performance of the $DSOGI$-based estimation architecture

TABLE I: Plant and Compensator Parameters

Parameter	Value
Power Rating	300 KVA
V_{dc}	450 V
R_o	−0.8 Ω
L_o	3.99 mH
C_o	0.001 763 F
k_v	0.1
k_i	−0.0001
R	1.0 Ω
L	4.2 mH
f_{sw}	20 kHz
v_{ac}	208 V(L − L))
R_c	80 Ω

IV. Results and Discussions

The presented system is modeled in MATLAB/Simulink and PLECS domain, and various case study results have proven

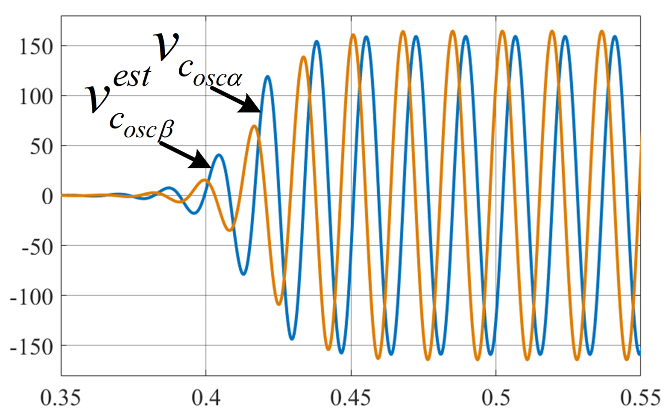

Fig. 4: Generated and estimated voltages from the VO-based architecture

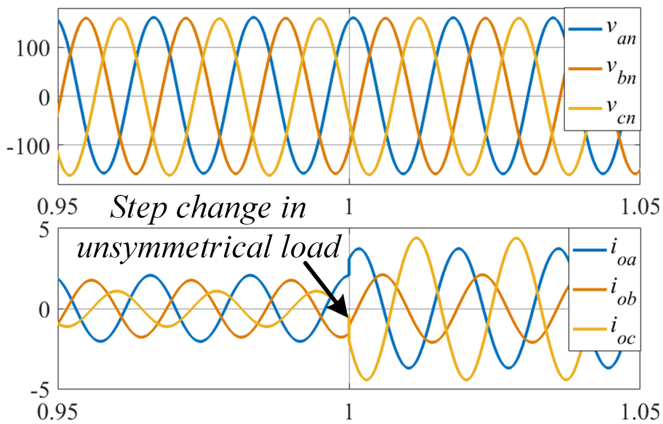

Fig. 5: Step change in unsymmetrical load at the converter terminals

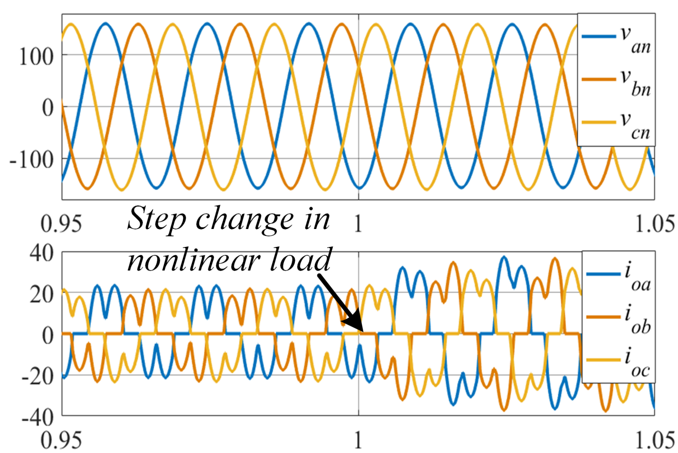

Fig. 6: Step change in nonlinear load at the converter terminals

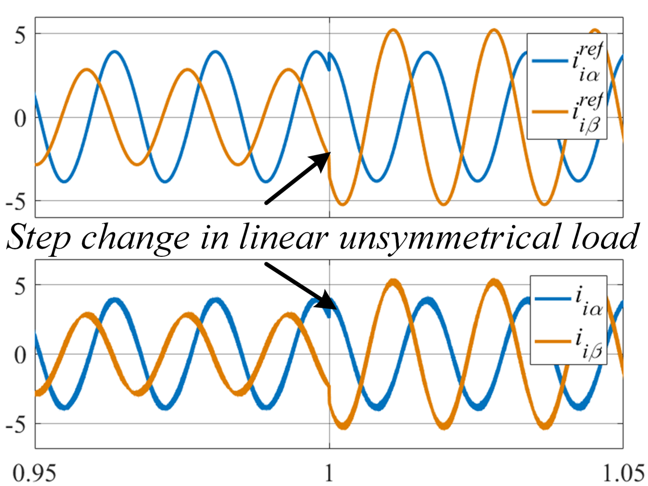

Fig. 7: Reference and actual current for step change in linear unsymmetrical load

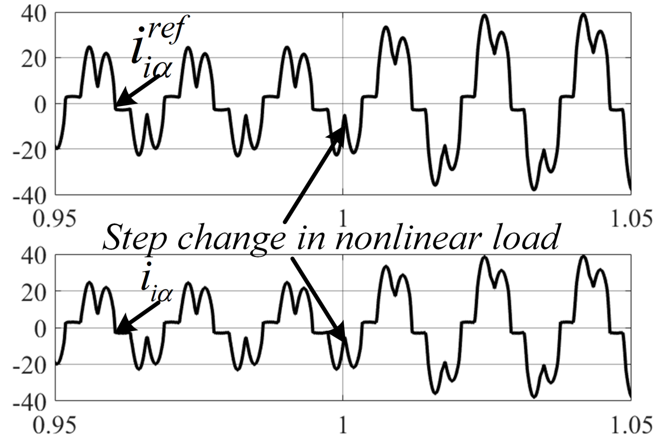

Fig. 8: Reference and actual current for step change in nonlinear load

the efficacy of the system. The values of the parameters for simulation are presented in Table I. The results showing the voltage buildup for both the α axis as well as the estimated oscillatory voltage of the β axis are presented in Fig. 4. From this result it is observed that with the chosen parameters of the oscillator, it is possible to accomplish voltage buildup. The result showing the operation of the overall system for a worst case transient of step change in unsymmetrical load is shown in Fig. 5, where a step change in the load is presented. This result shows that the architecture with the inner loop is able to successfully accomplish the overall control objective. The next result shows the terminal voltage and current during a step change with a nonlinear load as presented in Fig. 6. This result shows that it is still possible to maintain balanced low harmonic terminal voltage, which proves the efficacy of the proposed architecture. The next results show the reference and the actual currents from the inner loop for the α axis, as presented in Fig. 7 and Fig. 8 for linear and nonlinear loads, respectively. Similar results can also be obtained for the β axis. It is observed that the generated and actual currents in both the cases track each other with negligible difference, indicating the efficacy of the inner loop. The total harmonic distortion of the generated voltages from the VO are $< 5\%$, as prescribed in [23], indicating the efficacy of the overall system.

V. Conclusion

This paper presents a modified virtual oscillator with a Lyapunov energy function-based inner control loop. The dynamics of a Lienard type virtual oscillator with equivalent series RLC circuit representation has been accomplished in this paper. The parameters for this oscillator are chosen such that the fundamental frequency of the system remains at $60Hz$. It is observed from the results that during transients of load switching in grid-forming mode, the overall system is able to maintain low harmonic terminal voltage with unbalanced loading condition. Similar performance can be accomplished for the terminal voltage with nonlinear load step change. Finally, the reference and actual currents generated for the inner loops also track each other without any appreciable steady state errors, indicating the efficacy of the proposed approach.

References

[1] A. Timbus, M. Liserre, R. Teodorescu, P. Rodriguez, and F. Blaabjerg, "Evaluation of current controllers for distributed power generation systems," *IEEE Transactions on Power Electronics*, vol. 24, pp. 654–664, March 2009.

[2] F. Blaabjerg, R. Teodorescu, M. Liserre, , and A. V. Timbus, "Overview of control and grid synchronization for distributed power generation systems," *IEEE Transactions on Industrial Electronics*, vol. 53, pp. 1398–1409, October 2006.

[3] A. A. Nabulsi and R. Dhaouadi, "Efficiency optimization of a DSP based standalone PV system using fuzzy logic and dual-MPPT control," *IEEE Transactions on Industrial Informatics*, vol. 8, pp. 573–584, Aug 2012.

[4] S. B. Kjaer, J. K. Pedersen, and F. Blaabjerg, "A review of single-phase grid-connected inverters for photovoltaic modules," *IEEE Transactions on Industry Application*, vol. 41, pp. 1292–1306, Oct 2005.

[5] V. R. Chowdhury, S. Mukherjee, and J. W. Kimball, "A voltage sensorless control of a three phase grid connected inverter based on Lyapunov energy function under unbalanced grid voltage condition," in *Proc. 10th IEEE-ECCE.*, Portland, USA, September 2018.

[6] V. R. Chowdhury, "Enhanced operation of a virtual synchronous machine under unbalanced grid voltage condition based on lyapunov energy function," *IEEE Journal of Emerging and Selected Topics in Industrial Electronics*, Early Access.

[7] V. R. Chowdhury and D. Divan, "Control of soft switching solid state transformer based on lyapunov energy function for three-phase ac-ac power conversion," in *IECON 2021 – 47th Annual Conference of the IEEE Industrial Electronics Society*, Toronto, ON, Canada, November 2021.

[8] U. Datta, A. Kalam, and J. Shi, "Battery energy storage system control for mitigating pv penetration impact on primary frequency control and state-of-charge recovery," *IEEE Transactions on Sustainable Energy*, vol. 11, pp. 746–757, April 2020.

[9] N. Liu, Q. Chen, X. Lu, J. Liu, and J. Zhang, "A charging strategy for pv-based battery switch stations considering service availability and self-consumption of pv energy," *IEEE Transactions on Industrial Electronics*, vol. 62, pp. 4878–4889, August 2015.

[10] H. Komurcugil, N. Altin, S. Ozdemir, and I. Sefa, "Lyapunov-function and proportional-resonant-based control strategy for single-phase grid-connected VSI with LCL filter," *IEEE Transactions on Industrial Electronics*, vol. 63, pp. 2838–2849, May 2016.

[11] H. Komurcugil, "Improved passivity-based control method and its robustness analysis for single-phase uninterruptible power supply inverters," *IET Power Electronics*, vol. 8, pp. 1558–1570, Mar 2015.

[12] Q.-C. Zhong and G. Weiss, "Synchronverters: Inverters that mimic synchronous generators," *IEEE Transactions on Industrial Electronics*, vol. 58, pp. 1259–1267, April 2011.

[13] B. K. Poolla, Y. Lin, A. Bernstein, E. Mallada, and D. Groß, "Frequency shaping control for weakly-coupled grid-forming ibrs," *IEEE Control Systems Letters*, vol. 7, pp. 937–942, 2023.

[14] B. B. Johnson, S. V. Dhople, A. O. Hamadeh, and P. T. Krein, "Synchronization of parallel single-phase inverters with virtual oscillator control," *IEEE Transactions on Power Electronics*, vol. 29, no. 11, pp. 6124–6138, 2014.

[15] L. Zhang, L. Harnefors, and H.-P. Nee, "Power-synchronization control of grid-connected voltage-source converters," *IEEE Transactions on Power Systems*, vol. 25, pp. 809 – 820, May 2010.

[16] V. R. Chowdhury and A. Singh, "A nonlinear direct power controller for a three-phase grid-connected inverter with online parameter update for pv application," in *2022 IEEE Energy Conversion Congress and Exposition (ECCE)*, 2017, pp. 1–6.

[17] J. Noguchi, H. Tomiki, S. Kondo, and I. Takahashi, "Direct power control of PWM converter without power-source voltage sensors," *IEEE Transactions on Industry Applications*, vol. 34, pp. 473–479, May/Jun 1998.

[18] M. Malinowski, M. P. Kazmierkowski, S. Hansen, F. Blaabjerg, and G. D. Marques, "Virtual-flux-based direct power control of three-phase PWM rectifiers," *IEEE Transactions on Industry Applications*, vol. 37, pp. 1019–1027, Jul./Aug 2001.

[19] B. Johnson, M. Rodriguez, M. Sinha, and S. Dhople, "Comparison of virtual oscillator and droop control," in *2017 IEEE 18th Workshop on Control and Modeling for Power Electronics (COMPEL), Stanford, CA, USA*, pp. 1–6.

[20] H. Komurcugil, N. Altin, S. Ozdemir, and I. Sefa, "Lyapunov-function-based control strategy for single-phase ups inverters," *IEEE Transactions on Power electronics*, vol. 30, p. 3976–3983, July 2015.

[21] K. Hasan, "Passivity-based control of single-phase pwm current-source inverters," in *IECON 2007 - 33rd Annual Conference of the IEEE Industrial Electronics Society*, Taipei, Taiwan, November 2007.

[22] P. Rodriguez, R. Teodorescu, I. Candela, A. V. Timbus, M. Liserre, and F. Blaabjerg., "New positive-sequence voltage detector for grid synchronization of power converters under faulty grid conditions," in *Proc. 37th Annual IEEE Power Electronics Specialist Conf.*, Jeju, South Korea, June 2006.

[23] IEEE Standards Association, "IEEE standard for interconnection and interoperability of distributed energy resources with associated electric power systems interfaces," in *IEEE Std 1547-2018 (Revision of IEEE Std 1547-2003) - Redline*, 2018, p. 1–227.